

Spectral analysis of simulated Hall thruster discharge current oscillations

IEPC-2009-084

*Presented at the 31st International Electric Propulsion Conference,
University of Michigan, Ann Arbor, Michigan, USA
September 20–24, 2009*

Paul N. Giuliano* and Iain D. Boyd†
The University of Michigan, Ann Arbor, MI, 48109, USA

A hybrid fluid-PIC simulation code is employed in order to compare time-averaged and time-varying results to experimental measurements for a 6 kW Hall thruster. Time-averaged performance data from simulation and experiment are used to assess the response of the code under various operating conditions. Spectral analysis of simulated and experimental discharge current traces is also used to compare the time-varying nature of the discharge. While time-averaged performance data shows good correlation between simulation and experiment, time-varying results show many disparities. The simulation is operated using varying numerical parameters in order to observe any sensitivity in the results. While certain numerical parameters show little effect on time-averaged and time-varying results, other numerical parameters have a strong effect on the time-varying data which in turn changes the magnitudes and overall response of time-averaged results. These sensitivities of results to numerical parameters are probed and analyzed and point toward a high-frequency mode which is only captured when operating in a specific variation of the electron cross-field mobility model. In addition, deviations in this high-frequency mode are correlated to changes in simulation time step and relative length-scales of the mobility model. It is shown that this response may be a byproduct of the physical models of the simulation and the numerical scheme used to solve the plasma equations.

Nomenclature

I_d	= discharge current
F_{th}	= force due to thrust
f	= frequency
Δt	= base (ion) time step
Δt_e	= electron subcycle time step
m_a	= mass of species a
n_a	= number density of species a
q	= elementary charge
ν_a	= collision frequency for phenomenon a
μ_{ez}	= axial, cross-field electron mobility
α	= location-based scaling coefficient for electron mobility modeling
ω_a	= plasma frequency of species a
Z	= charge number
B_i	= magnetic field, i component

*Graduate Student, Department of Aerospace Engineering, pgiulian@umich.edu.

†Professor, Department of Aerospace Engineering, iainboyd@umich.edu.

I. Introduction

HALL thrusters are known to generate oscillation modes as a result of physical processes, some of which are known and others which are still being observed and studied,¹ making time-varying modeling an important research topic. For the past decade, the Hall thruster model HPHALL has been the focus of much research and development. HPHALL performs an axisymmetric simulation of the plasma within the thruster discharge chamber and near-field plume which employs both fluid and particle-in-cell (PIC) numerical methods.² The code has been found to be potentially effective in creating either time-averaged outputs of performance data which could be used, for example, as source terms into an erosion model,³ or to observe and analyze the time-varying nature of the detailed evolution of the internal plasma of a Hall thruster at small timescales.⁴ However, it seems that the time-varying results have undergone less scrutiny due to the fact that while time-averaged results are tunable for accurate steady-state comparisons to experiment, time-varying observations can be plagued with inconsistencies. It is this time-varying nature and subsequent phenomena of time-varying operation which is the focus of this paper.

This paper provides a brief introduction to the Hall thruster under consideration and the simulation code. The methods of comparison for the present work are outlined whereby simulated results of both performance and spectral analyses are compared to experimental results for assessment purposes. Assessment of the code's ability to replicate accurate performance output is shown to be successful for time-averaged data for the Hall thruster's operating conditions of interest. However, some of the numerical parameters used in the simulation of these operating conditions are shown to have adverse effects on the response of physical models. Varying responses due to physical models are then shown to have an effect on time-varying characteristics of the performance output. The results and disparities of this assessment demonstrate the consequent need for a more detailed look at numerical schemes of the physical models as well as the numerical parameters employed. Steps are taken to vary simulation particle population, time step, and the length scales of certain physical models in order to study the way in which time-varying data is affected.

II. Technical Approach

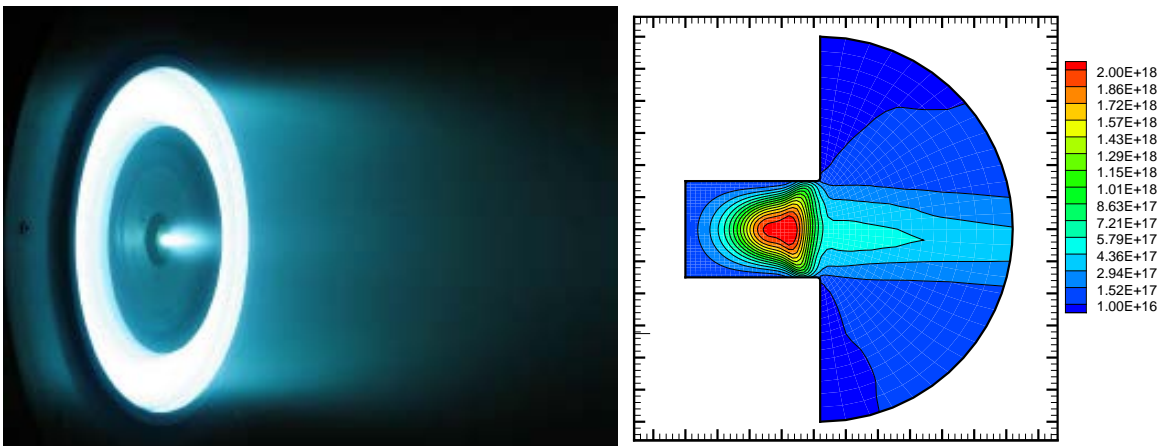


Figure 1. Photograph of the 6 kW Hall thruster in operation within the LVTF (Left) and simulated results of time-averaged, axisymmetric contours of electron number density (m^{-3}) (Right).

A. Hall Thruster and Experiments

The experiments used for the comparison purposes of this study were performed by Reid using a 6 kW laboratory model Hall thruster,⁵ seen in Figure 1. Experiments were performed in the Large Vacuum Test Facility (LVTF), a 6 m diameter by 9 m long cylindrical, stainless steel chamber with seven cryopumps, at the University of Michigan's Plasmadynamics and Electric Propulsion Laboratory (PEPL). The thruster was operated on a 100 kW power supply using a separate 1 kHz RC discharge filter for protection. Commercially available power supplies were used to power the cathode heater, cathode keeper, and magnet circuitry.

Research grade xenon propellant (99.999% pure) was used for cathode and anode supply. Nominal operating conditions are shown in Table 1.

In order to gather time-averaged discharge current data, a calibrated current shunt and multimeter were used in correlation with the main discharge power supply read-out. Time-varying discharge current data was gathered using a commercially available, high-speed current shunt rated for 100 kHz and placed on the cathode return line in between the thruster and RC filter.

B. Numerical Model

The computer code HPHALL performs an axisymmetric simulation which is commonly referred to as “hybrid-PIC”, utilizing fluid approximation equations in the treatment of electrons and a particle-in-cell (PIC) method in the treatment of heavy species, namely singly- and doubly-charged xenon ions and atoms. The electron equations are solved at a smaller time step, called the electron subcycle, in order to simulate how the speed of electrons is much faster than that of a heavy species. This allows for electron fluid equations to be fully solved and settled in between xenon particle updates. Hybrid fluid-particle methods have been shown to be successful in Hall thruster plume studies⁶ and are computationally cheaper than fully kinetic methods.⁷ The code was originally created by Fife and Martinez-Sánchez² and then later advanced by Gamero-Castaño and Katz to include such upgrades as a more detailed sheath model and a sputtering yield algorithm for the use as an erosion model.⁸ Parra et al. also made certain advances by way of improving such algorithms as heavy particle modeling, electron mobility modeling, plasma weighting, and ionization models, among others.^{4,9} Further development and corrections were performed by Hofer et al. on the heavy particle modeling, erosion sub-model, and electron mobility physics, continuing the development of the code to the present version.^{3,10–12} Through this past work, the code has a favorable history of presenting good agreement with macroscopic properties, such as discharge current and thrust, as well as local properties, such as plasma density, plasma potential, and electron temperature. An example of this time-averaged output of the code can be seen in Figure 1 which is a representation of electron number density at optimal operating conditions, detailed in the next section. For this type of two-dimensional contour plot, the anode is located on the left side and the near-field plume is located on the right side of the domain.

III. Results

A. Code Assessment

In order to assess the code using experimental results, simulations are performed at several different, physical operating conditions which are nominal to the thruster’s operation and explained in detail later. Simulations are performed by injecting neutral xenon into the domain, with plasma physics turned off, for approximately 1 ms of simulated time followed by approximately 4 ms of simulated time where the plasma physics are turned on. For example, when operating at the time step $\Delta t = 5 \times 10^{-8}$ sec, 20,000 iterations of neutral injection are followed by 80,000 iterations of plasma simulation. At these operating conditions, and using approximately 300,000 particles, this simulation requires about 12 hours of computer run time. All comparisons are performed with electron subcycles of either $0.01\Delta t$ or $0.001\Delta t$ which have little effect on either the time-averaged or time-varying solutions of the simulation. The electron subcycle is discussed further in the time step study section.

Table 1. Hall thruster operating conditions for both experiment and simulation for a discharge voltage of 300 V. The simulation marked with an asterisk (*) includes the facility background pressure.

Flowrate	I_d (A)	I_d (A)	% Diff.	F_{th} (N)	F_{th} (N)	% Diff.
	Experiment	HPHALL		Experiment	HPHALL	
10 mg/sec	9.06	8.82	2.6	0.185	0.175	5.4
20 mg/sec	19.94	19.80	0.7	0.398	0.394	1.0
20 mg/sec	19.94	19.88*	0.3	0.398	0.386*	3.0
30 mg/sec	33.80	32.14	4.9	0.620	0.599	3.4

1. Performance Comparison

Nominal experimental operating conditions include discharge voltages of 150 V, 300 V, and 600 V at mass flow rates of 10 mg/sec, 20 mg/sec, and 30 mg/sec. Simulations are run at all operating conditions but are focused on the optimal operating conditions of 300 V, 20 mg/sec. Simulated, time-averaged performance data are compared to experimental performance data. The two major comparisons being discharge current, I_d , and thrust, F_{th} , and show that simulated results are very accurate. This comparison of varying flowrate for the optimal discharge voltage of 300 V can be seen in Table 1. Included in Table 1 is the condition of added facility background pressure, an algorithm which injects neutral particles at the simulation boundary. This method brings performance output closer to experimental results and ultimately simulates a more accurate portrayal of the real system. The reason for the best agreement at optimal conditions is because of the internal tuning of electron mobility physics within the simulation which has been pre-set to show the best agreement with these optimal conditions, the conditions that the Hall thruster is designed for and at which it would most likely be operated. This time-averaged comparison shows very good agreement between simulation results and experimental measurement at the operating conditions of interest.

2. Spectral Comparison

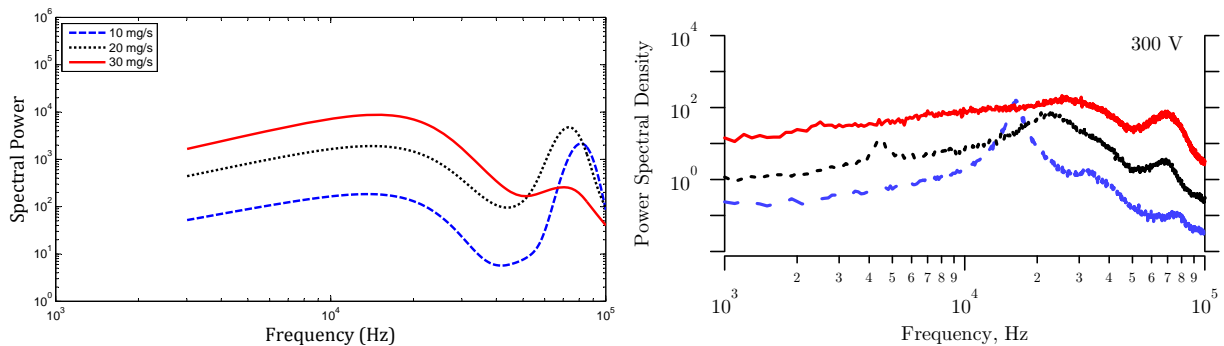


Figure 2. Power spectral density of simulation (Left) and experiment (Right) from Reid⁵ (Right).

Discharge oscillations from both simulation and experiment are also compared via power spectra. Simulated trends can be seen in the Hall thruster discharge current spectral power analysis found in Figure 2 and show relatively good agreement with experimental data,⁵ also found in Figure 2 (using the same color scheme for the purpose of comparison), though the agreement is far from exact. The noisy simulated data has been processed through a basic, one-dimensional smoothing algorithm for the purely observational purposes of comparing relative magnitudes and trends. In terms of absolute values, it is found that the model simulates a much larger magnitude discharge current oscillation than the experimental data. At optimal operating conditions, data from Reid⁵ report a standard deviation of the discharge oscillations as approximately 8% of the mean discharge current whereas the simulations show an approximately 8-25% oscillation (depending on time step size and mobility model, as will be shown later), which translates to approximately 25-50% in peak-to-peak terms. The familiar breathing mode oscillation appears in the range of 10-30 kHz in both spectra. A higher frequency mode is also clearly present at around 70-100 kHz although its source is not clear. While the fact that this mode is seen in both data sets seems like a potentially important finding, it will be shown that the computational result is sensitive to physical modeling and numerical parameters. These results give a glimpse into the details of such time-varying phenomena which will affect the validity of time-varying comparisons.

B. Effects of Electron Mobility Modeling

The first phenomena which must be discussed are the electron mobility models currently available within HPHALL and their effects on time-varying solutions. Cross-field electron mobility is modeled in the code as¹²

$$\mu_{ez} \simeq \frac{\nu_e m_e}{q B_r^2}, \quad (1)$$

a measure of the propensity for electrons to cross magnetic field lines axially rather than stay in an azimuthal drift within the discharge channel. The effective electron collision frequency, ν_e , is given by

$$\nu_e = \nu_{ei} + \nu_{en} + \nu_{\text{wall}} + \nu_{\text{bohm}} \quad (2)$$

with ν_{en} as the electron-neutral collision frequency, ν_{ei} as the electron-ion collision frequency, ν_{wall} as the collision frequency of the electrons with the walls, and ν_{bohm} as a collision frequency due to anomalous Bohm diffusion for electrons. The anomalous Bohm diffusion parameter is a user-augmented parameter which holds the purpose of matching simulated, effective collision frequencies with those of experimental measurements. Anomalous Bohm diffusion is modeled in the code as

$$\nu_{\text{bohm}} = \alpha \frac{1}{16} \omega_{ce} \quad (3)$$

where α is an arbitrary parameter adjusted to match experimental results by providing for the necessary location-based cross-field diffusion values. For example, the case for classical Bohm diffusion uses $\alpha = 1$. HPHALL was originally created with a single value for α and then moved to a two-region model, with separate values of α_c and α_p for the channel and the plume, respectively, after it was found that a two-region model shows an improvement in accuracy on similar but different codes.^{13,14} A three-region model was later implemented by Hofer et al.¹² in order to more closely align cross-field mobility to the distribution of the Hall parameter within the channel, separating the parameter into α_c , α_e , and α_p for the channel, acceleration region, and plume, respectively. A visual representation of the three-region mobility model can be seen in Figure 3. The previous, two-region model can also be visualized by combining Regions I and II of Figure 3. As used by Hofer et al. and in order to maintain consistency, in the present study values of $\alpha_c = 0.044$, $\alpha_p = 1$ are used for the two-region model and $\alpha_c = 0.08$, $\alpha_e = 0.016$, $\alpha_p = 10$ are used for the three-region model.

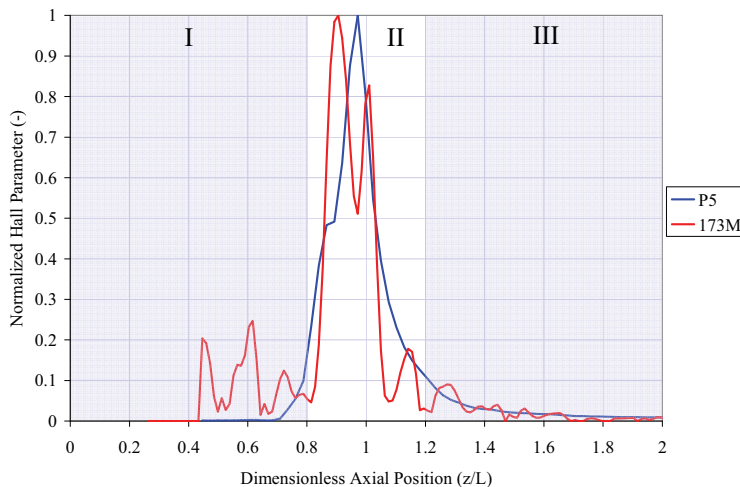


Figure 3. Experimental data of the Hall parameter versus axial position along with a representation of the different mobility regions within the simulation domain as portrayed by Hofer et al.¹² The discharge channel exit plane is located at $z/L = 1$.

The simulated discharge current traces of the three-region mobility model produce more easily distinguishable features than the two-region model results, shown in Figure 4 in which the three- and two-region mobility models are compared side by side. The three most profound phenomena found in the three mobility region current traces are the breathing mode oscillation, a higher-frequency mode called the “three-region artifact”, and the discharge current lag from the beam to the anode. Common to both mobility models are the lag and breathing mode oscillations. In addition, as mentioned earlier, the three-region model predicts a standard deviation in the discharge oscillations of about 8-25% of the mean discharge current while the two-region model predicts a steady deviation of approximately 8%. These relative magnitudes can be seen in the side by side comparison. The spectral analyses of two-region and three-region simulations can be found in Figure 5 for four different simulation time steps, showing significant differences in the results produced by

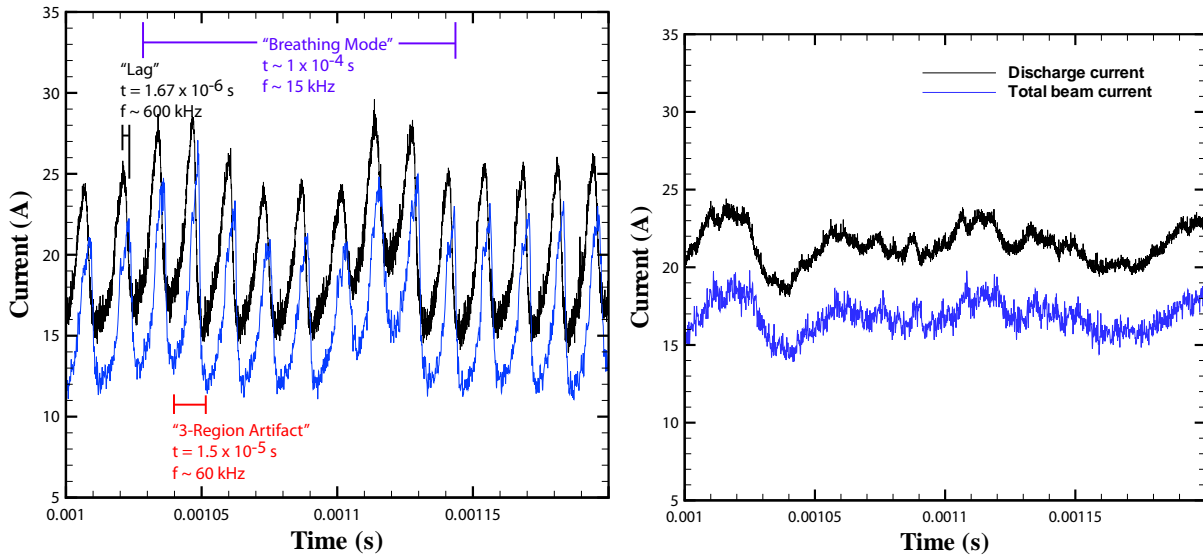


Figure 4. A comparison of simulated discharge and beam current profiles using the three-region (Left) and two-region (Right) mobility models. Notable phenomena are marked and labeled in the three-region trace.

the two mobility models. The time steps used in this parametric study are $\Delta t = 5 \times 10^{-9}$ sec, 2.5×10^{-8} sec, 5×10^{-8} sec, and 10×10^{-8} sec.

A major feature found in the three-region current traces is the high-frequency mode which has a timescale of about 1.5×10^{-5} sec, corresponding to a frequency range of about 60-80 kHz which can be identified as the sharp peaks in the spectra of Figure 5. This mode is completely absent in the two-region results. In addition, higher frequency harmonics due to the high-frequency mode are not observed in the larger time step of $\Delta t = 10 \times 10^{-8}$ sec, instead only displaying a single spectral spike. This indicates that the oscillation mechanism occurs at a timescale somewhere in between $\Delta t = 5 \times 10^{-8}$ sec and $\Delta t = 10 \times 10^{-8}$ sec.

C. Effects of Numerical Parameters

Despite the similarity of the power spectra trends between experiment and simulation for the 6 kW Hall thruster, it is found that certain numerical parameters greatly affect the simulated time-varying solutions (as previously portrayed by Figure 5) while the time-averaged solutions remain relatively unchanged. In addition, these varying results are mobility-model specific. Part of the evaluation process of the code is to study any sensitivity of the solutions to the numerical parameters. Simulation particle population, time step, and the acceleration region (region II) length scale of the mobility model are varied in order to characterize the different time-varying solutions.

1. Particle Population Study

Spectral analysis is performed on the discharge current signal at varying particle populations and the results are shown in Figure 6 in which the three-region mobility model is used. The numbers of both neutral and singly-charged xenon are varied and show no change or shift in spectral components at the Hall thruster oscillation modes of interest. Low frequency results cannot be explained but seem to be weakly coupled to particle population. However, it has been observed experimentally and speculated that one source of such low frequency oscillations, often called the “spoke” mode, is coupled to density nonuniformities and ionization processes.¹⁵ The spoke mode is impossible to capture in HPHALL because the phenomenon is inherently azimuthal while the simulation operates in a radial-axial, axisymmetric manner. At these varying ion and neutral populations, time-averaged results, as well as two- and three-region results, vary by a negligible amount.

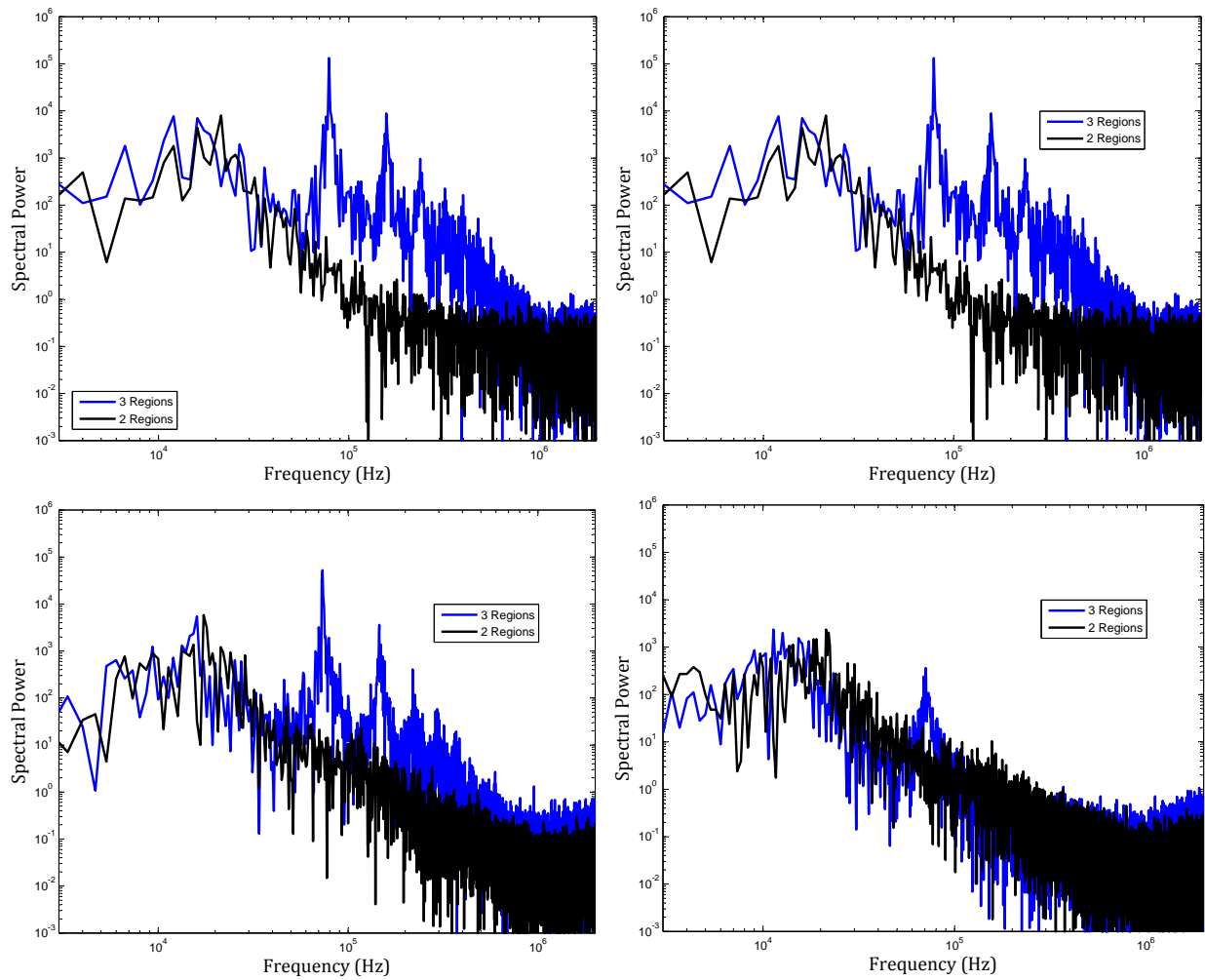


Figure 5. Spectral analyses from the two-region and three-region mobility models for time steps $\Delta t = 5 \times 10^{-9}$ sec (Top Left), 2.5×10^{-8} sec (Top Right), 5×10^{-8} sec (Bottom Left), and 10×10^{-8} sec (Bottom Right).

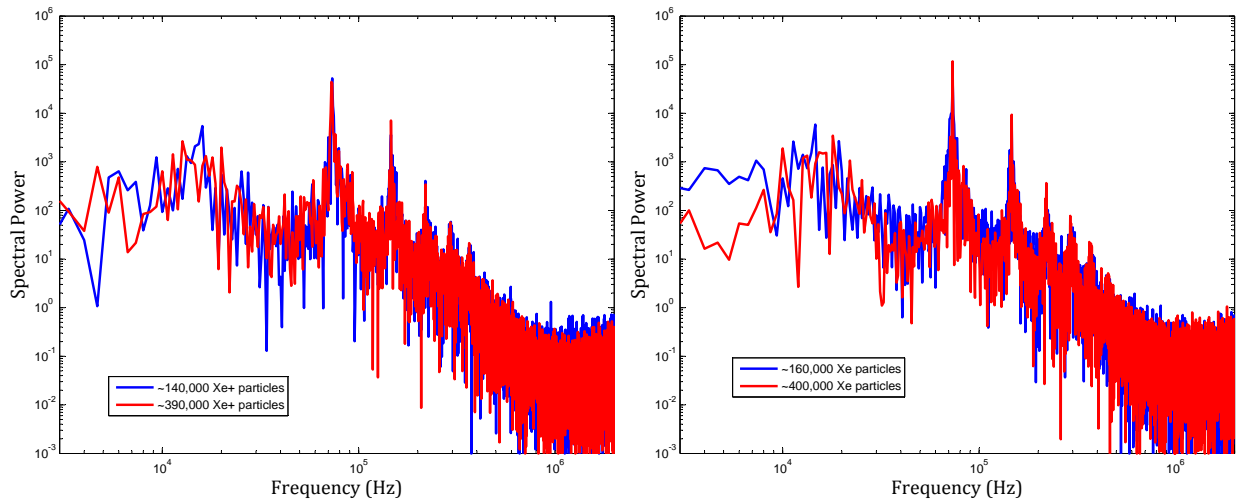


Figure 6. A comparison of power spectra obtained by varying singly-charged (Left) and neutral (Right) xenon particle populations with time step $\Delta t = 5 \times 10^{-8}$ sec using the three-region mobility model.

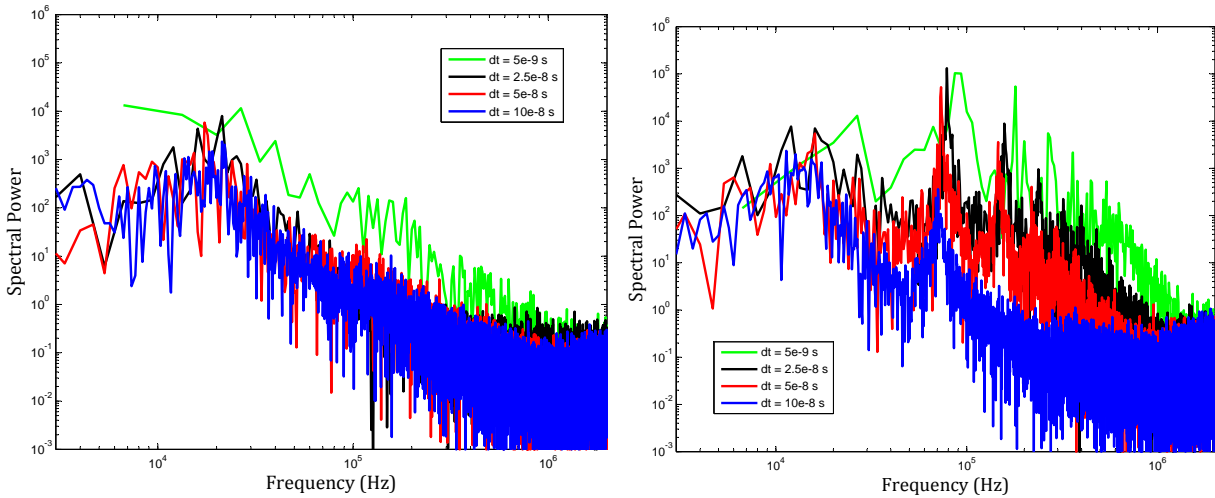


Figure 7. A comparison of power spectra obtained for varying time step within the two-region (Left) and three-region (Right) mobility simulation conditions.

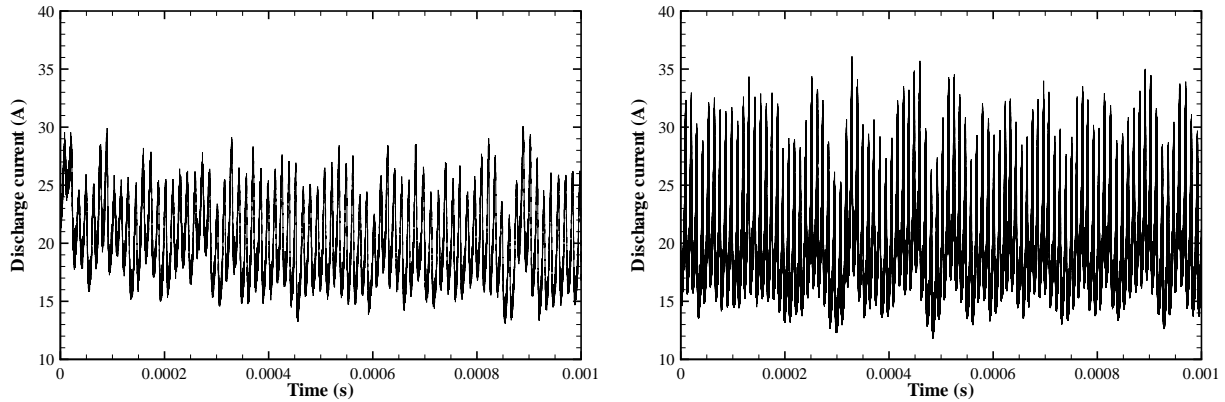


Figure 8. Simulated discharge current oscillations for time steps of 5×10^{-8} sec (Left) and 5×10^{-9} sec (Right) at optimal Hall thruster operating condition.

2. Time Step Study

Spectral analysis is also performed on the discharge current signals obtained with different time steps for both two-region and three-region simulations and the results are shown in Figure 7. At these different time steps, time-averaged results show significant changes in discharge current and thrust (see Table 2), one of the first indications of numerical sensitivity in the three-region mobility model. Table 2 also displays the very small difference in time-averaged results for varying electron subcycle. Decreasing time step shows a significant increase in the magnitude of the discharge current oscillations at higher frequencies when operating with the three-region model. This is not observed in the two-region simulations with the exception of the smallest time step, $\Delta t = 5 \times 10^{-9}$ sec, though the high-frequency mode is still not present. Furthermore, both the two-region and three-region models show similar trends in changing time-averaged data with decreasing time step, the trend in Table 2 showing increasing magnitudes until the smallest time step. Two simulated discharge current oscillations operating with the three-region mobility model and with an order of magnitude difference of simulation time step are shown side-by-side in Figure 8, displaying the magnitude increase and shift. It is also observed that the oscillations around the mean discharge current are not symmetric; the positive oscillations are of higher magnitude than the negative oscillations. The smaller time step simulations result in generally higher magnitude oscillations reaching peak-to-peak values on the order of about 50% the mean discharge current value, as mentioned before.

In order to verify that the simulation time steps are appropriate, electron and ion frequencies are calcu-

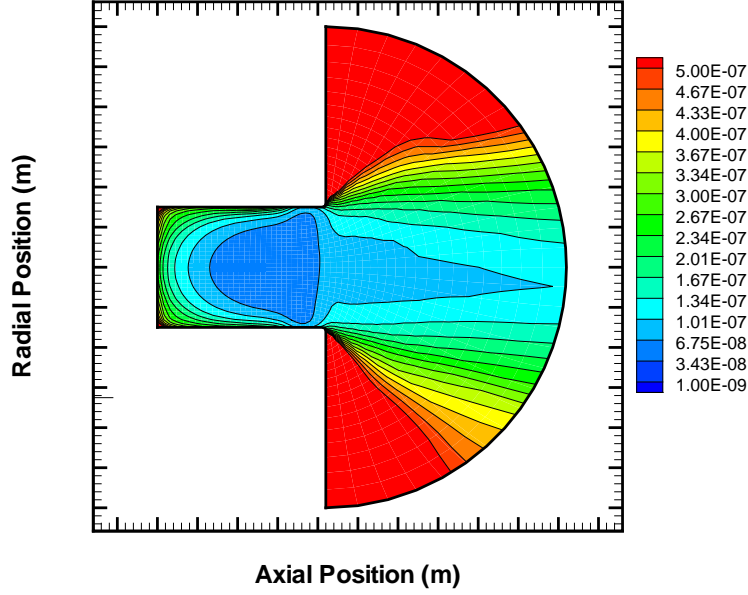


Figure 9. Two dimensional, time-averaged contours of local ion timescales.

Table 2. Simulated, time-averaged performance data for varying time step and subcycle in the three-region mobility model.

$\Delta t_e = 0.01\Delta t$			$\Delta t_e = 0.001\Delta t$		
Δt	I_d (A)	F_{th} (N)	Δt	I_d (A)	F_{th} (N)
5×10^{-9} sec	19.72	0.377	5×10^{-9} sec	19.69	0.377
2.5×10^{-8} sec	20.12	0.387	2.5×10^{-8} sec	20.14	0.388
5×10^{-8} sec	19.86	0.389	5×10^{-8} sec	19.98	0.391
10×10^{-8} sec	19.09	0.390	10×10^{-8} sec	19.12	0.390

lated¹⁶ using Equations 4 and 5. These frequencies correspond to ion timescales of approximately 1×10^{-9} sec to 5×10^{-7} sec, seen in Figure 9, and electron timescales which are approximately 500 times smaller. Despite this difference, it is important to note that at the larger electron subcycle, $\Delta t_e = 0.01\Delta t$, solutions still show little to no disparity.

More than an order of magnitude difference in time scale occurs between the bulk of the discharge within the channel and the near-plume region. These results show that the two smallest time steps, 5×10^{-9} sec and 2.5×10^{-8} sec, are small enough to capture macroscopic plasma phenomena throughout the whole domain. The 5×10^{-8} sec time step seems small enough yet very close to the timescales within the bulk discharge in the channel. The 10×10^{-8} sec time step is too large to resolve the detailed properties of the channel discharge (the bluest contours in Figure 9). This reinforces the previous observation that some of the high-frequency modes present in the spectral analyses of the smaller time steps are missing in the 10×10^{-8} sec studies.

$$\omega_e \equiv \left(\frac{4\pi n_e q^2}{m_e} \right)^{1/2} \quad (4)$$

$$\omega_i \equiv \left(\frac{4\pi n_i Z^2 q^2}{m_i} \right)^{1/2} \quad (5)$$

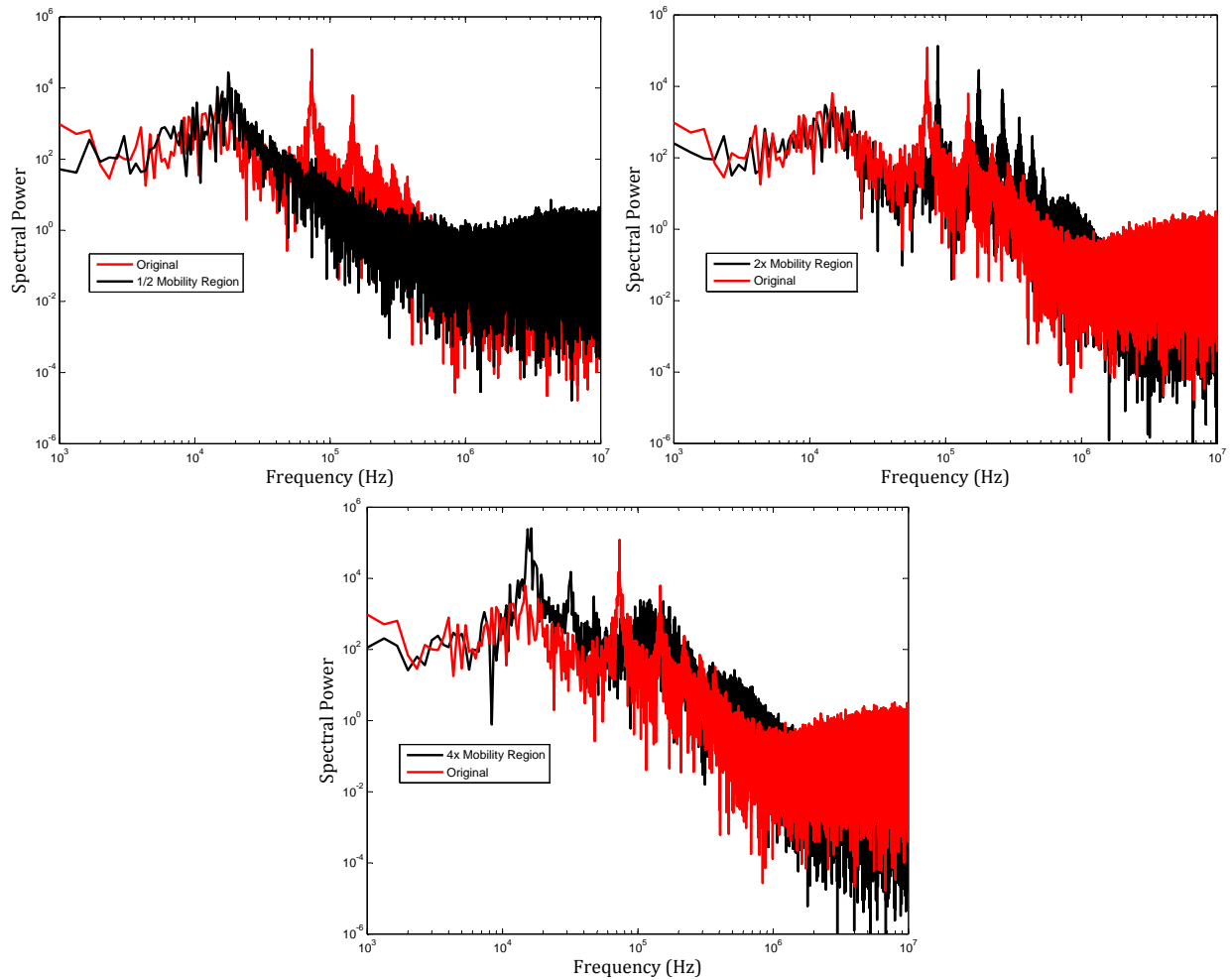


Figure 10. Spectral analyses from the three-region mobility model for half (Top Left), double (Top Right) and four times (Bottom) the original size of region II.

3. Mobility Region Length Study

Spectral analysis is also performed on the discharge current signals obtained with different lengths of region II of the three-region simulations and the results are shown in Figure 10. At these different lengths, time-averaged results show significant changes in discharge current and thrust (see Table 3). Firstly, it is important to note that without proper tuning of the mobility coefficient, α , time-averaged data from differing mobility regions will rarely match well. The purpose of changing mobility region lengths is primarily to observe any response of the high-frequency mode so that further analysis can be made of its physical nature.

Changing the acceleration region to half its original size (top left of Figure 10) results in a loss of the high-frequency mode, possibly because of the inability to resolve the physics introduced in this region. Doubling the size of region II (top right of Figure 10) shifts the high-frequency modes approximately 15 kHz higher. Increasing the size of region II to four times the original length (bottom of Figure 10) creates a sharper spike and resonances at the breathing mode and a broader bump centered at about 100 kHz. The responses of both time-averaged and time-varying data with varying mobility region size shows that the physical nature of the high-frequency mode might very well be associated with the physics captured by sizing the mobility regions to experimentally observed Hall thruster data, as previously portrayed by Figure 3.

Table 3. Simulated, time-averaged performance data for varying acceleration region of the three-region mobility model.

Region II Size	I_d (A)	F_{th} (N)
Original	19.98	0.391
Half	22.48	0.404
Double	17.04	0.351
$\times 4$	15.86	0.342

IV. Conclusion

Numerical modeling of a 6kW Hall thruster has been performed using an established hybrid fluid-PIC simulation code. Comparisons of numerical results to measurements of time-averaged properties such as thrust and discharge current showed very good agreement. However, the same solutions showed relatively poor agreement with measurements of discharge current oscillations. In particular, the simulations predicted higher magnitude oscillations than those observed experimentally.

Subsequent numerical studies investigated the sensitivity of the solutions in the time domain to the numerical parameters and electron mobility models employed. It was found that the results were insensitive to the number of particles employed. Significant sensitivity of the solutions to the time step employed was found, particularly for the three region mobility model. In addition, it was found that the length scales employed by the three-region mobility model affect the way in which the high-frequency mode is captured.

Future work will focus on the development of identifying guidelines that allow solutions to be computed that are independent of the numerical parameters employed. In addition, attempts will be made to modify the three-region electron mobility model to make its solutions less sensitive to numerical parameters. The methods used to simulate the detailed plasma physics within the discharge channel must eventually be improved to result in a more robust response to varying numerical parameters and physical models.

Acknowledgments

The research described in this paper was performed at the Nonequilibrium Gas and Plasma Dynamics Laboratory of the University of Michigan under the funding of AFOSR Grant Number FA9550-07-1-0274.

We would like to thank Rich Hofer at the Jet Propulsion Laboratory, California Institute of Technology, and Bryan Reid of the Plasmadynamics and Electric Propulsion Laboratory at the University of Michigan for their help and insight into numerical modeling of the 6 kW Hall thruster.

References

- ¹Choueiri, E., "Plasma oscillations in Hall thrusters," *Physics of Plasmas*, Vol. 8, No. 4, April 2001, pp. 1411–1426.
- ²Fife, J., *Hybrid-PIC Modeling and Electrostatic Probe Survey of Hall Thruster*, Ph.D. thesis, Massachusetts Institute of Technology, 1998.
- ³Hofer, R. R., Mikellides, I. G., Katz, I., and Goebel, D. M., "BPT-4000 Hall Thruster Discharge Chamber Erosion Model Comparison with Qualification Life Test Data," *30th International Electric Propulsion Conference, Florence, Italy*, , No. IEPC 2007-267, 2007.
- ⁴Parra, F., Ahedo, E., Fife, J., and Martinez-Sanchez, M., "A two-dimensional hybrid model of the Hall thruster discharge," *Journal of Applied Physics*, Vol. 100, No. 023304, 2006.
- ⁵Reid, B., *The Influence of Neutral Flow Rate in the Operation of Hall Thrusters*, Ph.D. thesis, The University of Michigan, 2009.
- ⁶Boyd, I. D., "Review of Hall Thruster Plume Modeling," *Journal of Spacecraft and Rockets*, Vol. 38, No. 3, 2001, pp. 381–387.
- ⁷Szabo, J., *Fully kinetic numerical modeling of a plasma thruster*, Ph.D. thesis, Massachusetts Institute of Technology, 2001.
- ⁸Gamero-Castano, M. and Katz, I., "Estimation of Hall Thruster Erosion Using HPHall," *29th International Electric Propulsion Conference, Princeton University, Princeton, NJ*, , No. IEPC 2005-303, 2005.
- ⁹Parra, F., Escobar, D., and Ahedo, E., "Improvements on particle accuracy in a Hall thruster hybrid code," *42nd AIAA/ASME/SAE/ASEE Joint Propulsion Conference, Sacramento, CA*, , No. AIAA 2006-4830, 2006.
- ¹⁰Hofer, R. R., Katz, I., Mikellides, I. G., and no, M. G.-C., "Heavy Particle Velocity and Electron Mobility Modeling

in Hybrid-PIC Hall Thruster Simulations,” *42nd AIAA/ASME/SAE/ASEE Joint Propulsion Conference, Sacramento, CA*, , No. AIAA 2006-4658, 2006.

¹¹Hofer, R. R., Mikellides, I. G., Katz, I., , and Goebel, D. M., “Wall Sheath and Electron Mobility Modeling in Hybrid-PIC Hall Thruster Simulations,” *43rd AIAA/ASME/SAE/ASEE Joint Propulsion Conference, Cincinnati, OH*, , No. AIAA 2007-5267, 2007.

¹²Hofer, R. R., Katz, I., Mikellides, I. G., Goebel, D. M., Jameson, K. K., Sullivan, R. M., and Johnson, L. K., “Efficacy of Electron Mobility Models in Hybrid-PIC Hall Thruster Simulations,” *44th AIAA/ASME/SAE/ASEE Joint Propulsion Conference, Hartford, CT*, , No. 2008-4924, 2008.

¹³Hagelaar, G. J. M., Bareilles, J., Garrigues, L., and Bouef, J. P., “Role of Anomalous Electron Transport in a Stationary Plasma Thruster Simulation,” *Journal of Applied Physics*, Vol. 13, No. 1, 2003, pp. 67–75.

¹⁴Koo, J. W. and Boyd, I. D., “Modeling of Anomalous Electron Mobility in Hall Thrusters,” *Physics of Plasmas*, Vol. 13, No. 033501, 2006.

¹⁵James, G. and Lowder, R., “Anomalous Electron Diffusion and Ion Acceleration in a Low-Density Plasma,” *Physics of Fluids*, Vol. 9, No. 1115, 1966.

¹⁶Nicholson, D. R., *Introduction to Plasma Theory*, John Wiley & Sons, Inc., 1983.